FT-IR (Nicolet 6700 FT-IR Spectrometer with SmartOrbit™ diamond ATR accessory in the range of 4000–400 cm^{-1}):

1: 3116 (w), 3109 (w), 3086 (w), 3053 (w), 3018 (w), 1616 (w), 1593 (m), 1583 (m), 1552 (w), 1506 (s), 1471 (w), 1456 (w), 1432 (m), 1381 (m), 1364 (m), 1335 (m), 1316 (w), 1302 (m), 1214 (m), 1176 (m), 1163 (w), 1145 (s), 1135 (m), 1104 (m), 1049 (w), 997 (w), 973 (m), 956 (m), 891 (w), 872 (m), 833 (vs), 802 (w), 783 (vs), 747 (vs), 701 (m), 658 (m), 650 (m), 635 (m), 623 (m), 525 (w), 500 (m), 487 (s)

2: 3115 (w), 3108 (w), 3086 (w), 3053 (w), 3016 (w), 1616 (w), 1593 (m), 1582 (m), 1552 (w), 1506 (s), 1471 (w), 1454 (w), 1433 (m), 1381 (m), 1363 (m), 1334 (m), 1316 (w), 1301 (m), 1214 (m), 1174 (m), 1162 (w), 1144 (s), 1134 (m), 1103 (m), 1048 (w), 996 (m), 973 (m), 956 (m), 892 (w), 872 (m), 832 (vs), 802 (w), 783 (vs), 747 (vs), 700 (m), 658 (m), 649 (m), 635 (m), 622 (m), 525 (w), 500 (m), 487 (s)

3: 3113 (w), 3106 (w), 3080 (w), 3047 (w), 3012 (w), 1615 (w), 1593 (m), 1581 (m), 1552 (w), 1505 (s), 1471 (w), 1455 (w), 1429 (m), 1380 (m), 1362 (m), 1334 (m), 1315 (w), 1299 (m), 1213 (m), 1173 (m), 1162 (w), 1143 (s), 1134 (m), 1102 (m), 1047 (w), 992 (m), 973 (m), 954 (m), 891 (w), 870 (m), 830 (vs), 800 (w), 781 (vs), 745 (vs), 698 (m), 657 (m), 648 (m), 635 (m), 622 (m), 524 (w), 498 (m), 485 (s)

Table S1 Crystal data and final refinement parameters for **1-3**

		1	**2**	**3**
Empirical formula		$C_{18}H_{12}N_2CoCl_2$	$C_{18}H_{12}N_2CoBr_2$	$C_{18}H_{12}N_2CoI_2$
Formula weight M_r		386.1	475.0	569.1
Temperature		120 K	120 K	120 K
Wavelength [Å]		1.54184	1.54184	1.54184
Crystal system		Monoclinic	Monoclinic	Monoclinic
Space group		$P2_1/c$	$P2_1/c$	$P2_1/c$
Unit cell dimensions	a [Å]	7.8402(3)	7.7948(2)	7.7734(2)
	b [Å]	12.2014(4)	12.3160(3)	12.5186(4)
	c [Å]	16.8762(6)	17.2656(4)	17.9276(7)
	β [°]	104.098(4)	102.812(2)	101.346(3)
Volume [Å^3]		1565.78(10)	1616.24(7)	1710.48(10)
Z		4	4	4
Density (calculated) [g/cm^3]		1.6381	1.9523	2.2097
Absorption coefficient [mm^{-1}]		11.714	14.100	36.194
Crystal dimensions [mm]		0.31×0.07×0.02	0.65×0.07×0.04	0.42×0.07×0.02
Θ range for data collection [°]		4.52 - 67.06	4.45 - 66.9	5 - 66.87
Reflections collected		12022	19218	13110
Independent reflections		2778	2870	3024
R(int)		0.0426	0.0427	0.0421
Completeness to Θ_{max} [%]		0.99	0.99	0.99
Absorption correction		Gaussian	Gaussian	Gaussian
Max. and min. transmission		0.234; 0.773	0.098; 0.589	0.053; 0.512
Data / restraints / parameters		2778 / 0 / 208	2870 / 0 / 208	3024 / 0 / 208
Goodness-of-fit on F^2		1.01	1.09	1.47
Final R indices [$I>2\sigma(I)$]	$R1$	0.0267	0.0202	0.0413
	$wR2$	0.0302	0.0247	0.1040
Final R indices (all data)	$R1$	0.0318	0.0226	0.0470
	$wR2$	0.0327	0.0258	0.1090

Table S2 Selected geometric parameters [Å, °] for **1-3**.

	1 (X = Cl)	**2** (X = Br)	**3** (X = I)
Co1–N1	2.0311(19)	2.029(2)	2.031(6)
Co1–N2	2.0362(17)	2.0378(19)	2.031(6)
Co1–X1	2.2275(7)	2.3642(5)	2.5520(12)
Co1–X2	2.2176(6)	2.3472(4)	2.5255(10)
N1–Co1–N2	81.70(7)	81.88(8)	81.9(2)
X1–Co1–X2	117.36(3)	117.864(18)	118.29(5)
N1–Co1–X1	114.45(5)	114.21(6)	115.23(16)
N1–Co1–X2	112.17(5)	112.30(5)	112.05(14)
N2–Co1–X1	107.67(5)	108.53(6)	109.33(15)
N2–Co1–X2	118.42(5)	116.78(6)	114.56(15)

Table S3 Possible hydrogen bonding interactions [Å, °] for **1**

D-H···A	d(D-H)	d(H···A)	d(D···A)	<(DHA)
C12-H1C12···Cl2^{i}	0.96	2.76	3.426(2)	128
C22-H1C22···Cl1^{i}	0.96	2.77	3.603(2)	145

Symmetry codes: (i) x, 3/2 – y, – ½ + z

Table S4 Possible hydrogen bonding interactions [Å, °] for **2**‡

D-H···A	d(D-H)	d(H···A)	d(D···A)	<(DHA)
C12-H1C12···Br2^{ii}	0.96	2.83	3.531(2)	131

Symmetry codes: (ii) x, ½ – y, – ½ + z

‡ the shortest contact for the Br1 bromido ligand, C22-H1C22···Br1^{ii} (d(H···A) = 2.99 Å and d(D···A) = 3.783(2) Å) is outside the usual range for hydrogen bonding interactions (d(H···Br) ≤ 2.88 Å).

Table S5 Possible hydrogen bonding interactions [Å, °] for **3**‡

D-H···A	d(D-H)	d(H···A)	d(D···A)	<(DHA)
C12-H1C12···I2^{ii}	0.96	2.97	3.724(7)	137

Symmetry codes: (ii) x, ½ – y, – ½ + z

‡ the shortest contact for the I1 iodido ligand, C22-H1C22···I1^{ii} (d(H···A) = 3.41 Å and d(D···A) = 4.131(7) Å) is outside the usual range for hydrogen bonding interactions (d(H···I) ≤ 3.03 Å).

Table S6 Possible π-π interactions [Å, °] for **1**

Cg(I)···Cg(J) ‡	d(Cg···Cg)	α	β	γ
Cg1···Cg1^{iii}	3.4941(12)	0	20.40	20.40
Cg1···Cg3^{iii}	3.5788(13)	0.66(11)	24.25	23.59
Cg2···Cg2^{iv}	3.7204(13)	0	23.70	23.70
Cg2···Cg4^{iv}	3.7172(14)	0.15(11)	23.82	23.87
Cg4···Cg4^{v}	3.4891(14)	0	14.26	14.26

Symmetry codes: (iii) 2 – x, 2 – y, – z; (iv) 2 – x, 1 – y, – z; (v) 1 – x, 1 – y, – z

Table S7 Possible π-π interactions [Å, °] for **2**

Cg(I)···Cg(J) ‡	d(Cg···Cg)	α	β	γ
Cg1···Cg1^{v}	3.4942(14)	0	20.56	20.56
Cg1···Cg3^{v}	3.6173(14)	0.82(11)	25.84	25.02
Cg2···Cg2^{vi}	3.7187(14)	0	22.28	22.28
Cg2···Cg4^{vi}	3.6991(14)	0.40(11)	22.18	21.80
Cg4···Cg4^{vii}	3.4955(14)	0	16.39	16.39

Symmetry codes: (v) 1 – x, 1 – y, – z; (vi) 1 – x, – y, – z; (vii) – x, – y, – z

Table S8 Possible π-π interactions [Å, °] for **3**

Cg(I)···Cg(J) ‡	d(Cg···Cg)	α	β	γ
Cg1···Cg1^{iv}	3.521(4)	0	20.85	20.85
Cg1···Cg3^{iv}	3.642(4)	0.9(3)	25.86	25.07
Cg2···Cg2^{viii}	3.648(4)	0	18.87	18.87
Cg2···Cg4^{viii}	3.663(4)	0.4(3)	20.03	19.81
Cg4···Cg4^{vi}	3.520(4)	0	19.05	19.05

Symmetry codes: (iv) 2 – x, 1 – y, – z; (vi) 1 – x, – y, – z; (viii) 2 – x, – y, – z

‡Cg1 represents the centroid of the heterocyclic ring containing N1 atom
Cg2 represents the centroid of the heterocyclic ring containing N2 atom
Cg3 represents the centroid of the carbocyclic ring containing C18 atom
Cg4 represents the centroid of the carbocyclic ring containing C28 atom
α denotes the dihedral angle between planes I and J;
β denotes the angle between the Cg(I)···Cg(J) vector and normal to plane I;
γ denotes the angle between the Cg(I)···Cg(J) vector and normal to plane J.

Table S9 The shortest C···C contacts [Å] between carbon atoms of 2,2'-biquinoline for **1-3**

	1		**2**		**3**
C(I)···C(J)	d(C···C)	C(I)···C(J)	d(C···C)	C(I)···C(J)	d(C···C)
C11···C15^{iii}	3.283(3)	C11···C15^{v}	3.279(3)	C11···C15^{iv}	3.311(9)
C13···C19^{iii}	3.280(3)	C13···C19^{v}	3.269(3)	C13···C19^{iv}	3.293(9)
C15···C11^{iii}	3.283(3)	C15···C11^{v}	3.279(3)	C15···C11^{iv}	3.311(9)
C19···C13^{iii}	3.280(3)	C19···C13^{v}	3.269(3)	C19···C13^{iv}	3.293(9)
C11···C26^{iv}	3.324(3)	C11···C26^{vi}	3.344(3)	C24···C26^{vi}	3.341(10)
C22···C28^{iv}	3.399(3)	C22···C28^{vi}	3.426(3)	C26···C24^{vi}	3.341(10)
C26···C11^{iv}	3.324(3)	C26···C11^{vi}	3.344(3)		
C28···C22^{iv}	3.399(3)	C28···C22^{vi}	3.426(3)		

Symmetry codes: (iii) 2 – x, 2 – y, – z; (iv) 2 – x, 1 – y, – z; (v) 1 – x, 1 – y, – z; (vi) 1 – x, – y, – z

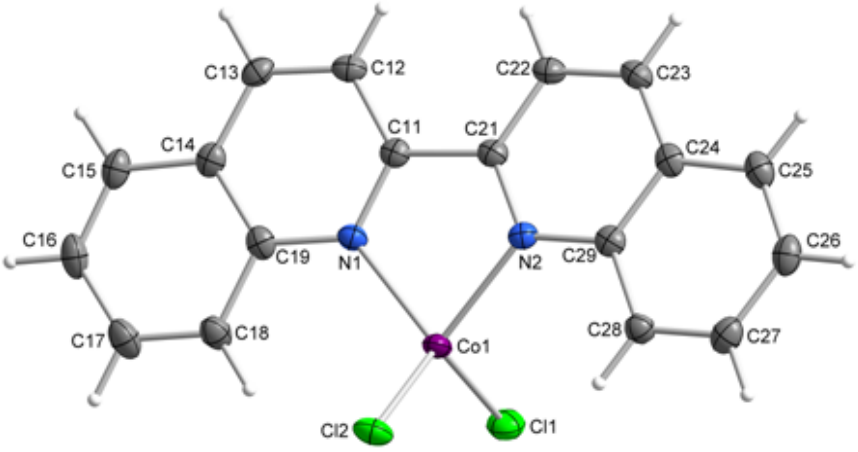

Fig. S1 Thermal ellipsoid plot of **1** showing the numbering scheme. The ellipsoids are drawn at 50 % probability level.

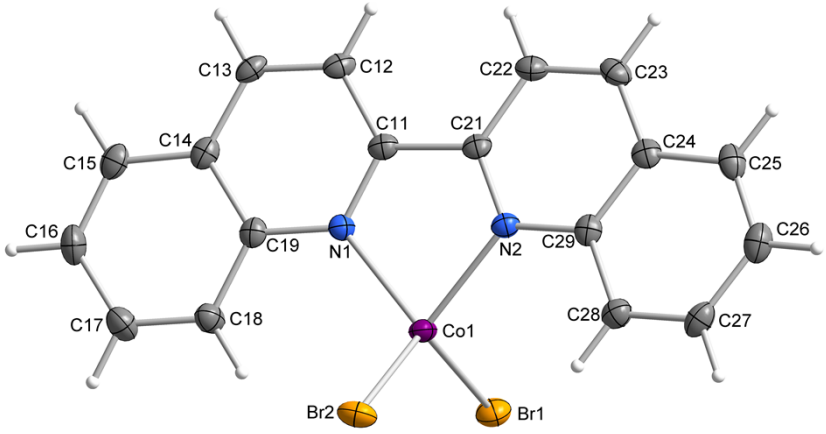

Fig. S2 Thermal ellipsoid plot of **2** showing the numbering scheme. The ellipsoids are drawn at 50 % probability level.

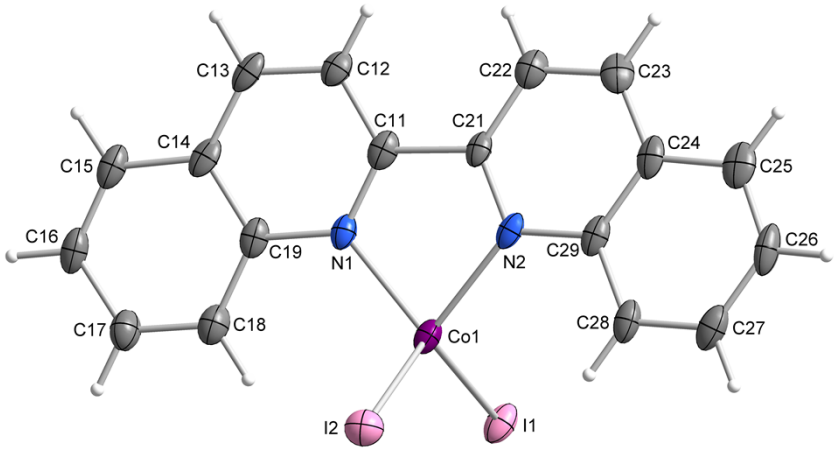

Fig. S3 Thermal ellipsoid plot of 3 showing the numbering scheme. The ellipsoids are drawn at 50 % probability level.

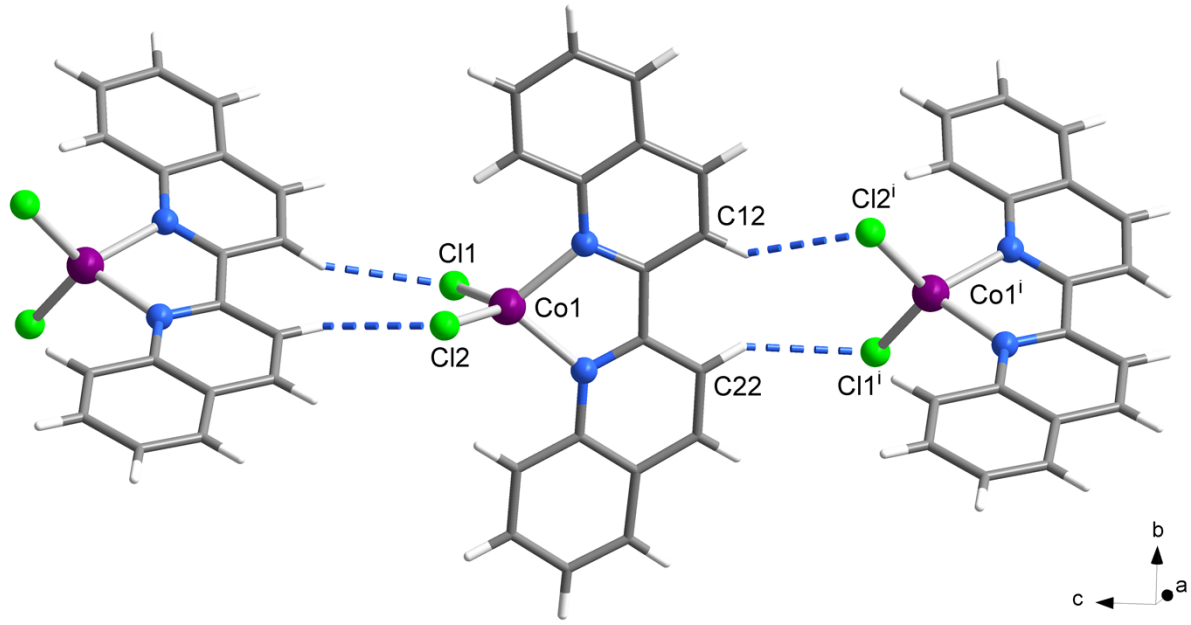

Fig. S4 Chain-like arrangement formed by weak C-H···Cl hydrogen bonding interactions of the complex molecules in **1**. Symmetry codes: (i) x, 3/2 – y, – ½ + z

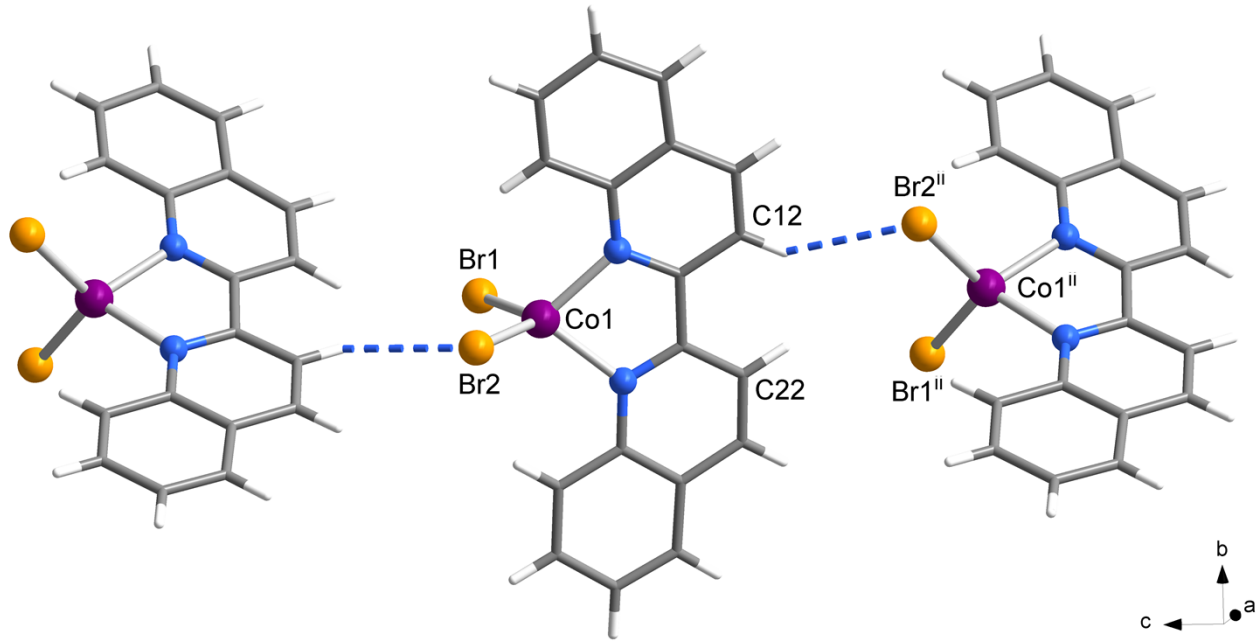

Fig. S5 Chain-like arrangement formed by weak C-H···Br hydrogen bonding interactions of the complex molecules in **2**. Symmetry codes: (ii) x, 3/2 – y, – ½ + z

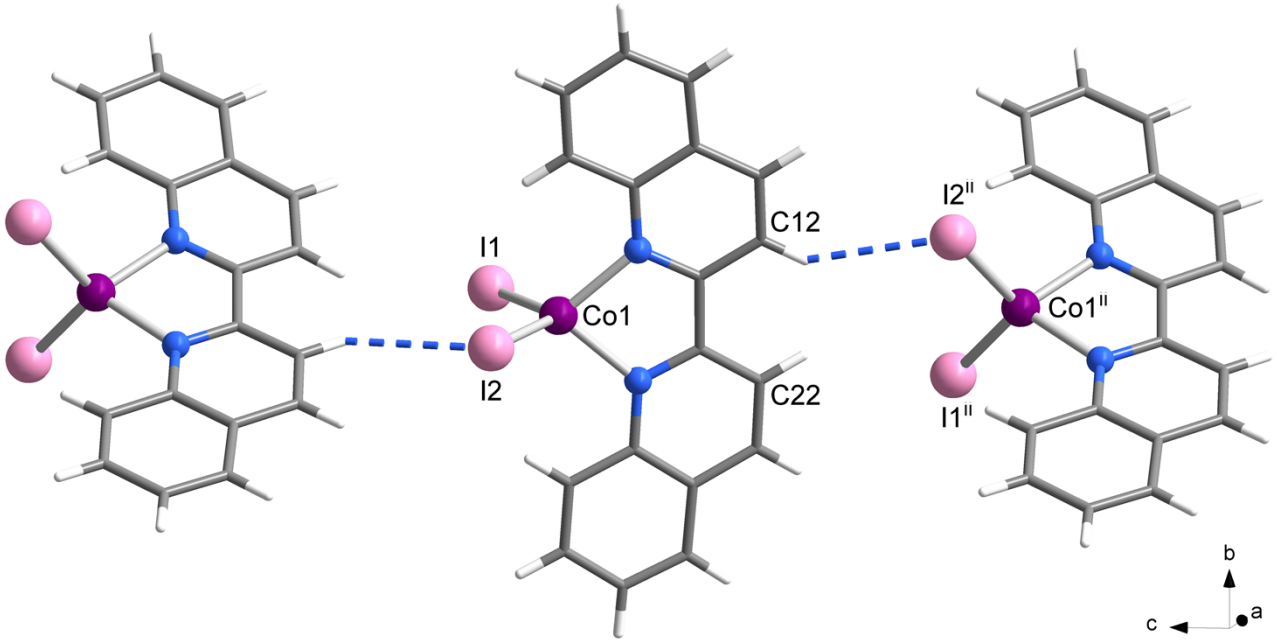

Fig. S6 Chain-like arrangement formed by weak C-H···I hydrogen bonding interactions of the complex molecules in **3**. Symmetry codes: (ii) x, 3/2 – y, – ½ + z

Table S10 The shortest C···C contacts [Å] between carbon atoms of 2,2'-biquinoline for **1-3**

	1		**2**		**3**
C(I)···C(J)	d(C···C)	C(I)···C(J)	d(C···C)	C(I)···C(J)	d(C···C)
C11···C15^{iii}	3.283(3)	C11···C15^{v}	3.279(3)	C11···C15^{iv}	3.311(9)
C13···C19^{iii}	3.280(3)	C13···C19^{v}	3.269(3)	C13···C19^{iv}	3.293(9)
C15···C11^{iii}	3.283(3)	C15···C11^{v}	3.279(3)	C15···C11^{iv}	3.311(9)
C19···C13^{iii}	3.280(3)	C19···C13^{v}	3.269(3)	C19···C13^{iv}	3.293(9)
C11···C26^{iv}	3.324(3)	C11···C26^{vi}	3.344(3)	C24···C26^{vi}	3.341(10)
C22···C28^{iv}	3.399(3)	C22···C28^{vi}	3.426(3)	C26···C24^{vi}	3.341(10)
C26···C11^{iv}	3.324(3)	C26···C11^{vi}	3.344(3)		
C28···C22^{iv}	3.399(3)	C28···C22^{vi}	3.426(3)		

Symmetry codes: (iii) 2 – x, 2 – y, – z; (iv) 2 – x, 1 – y, – z; (v) 1 – x, 1 – y, – z; (vi) 1 – x, – y, – z

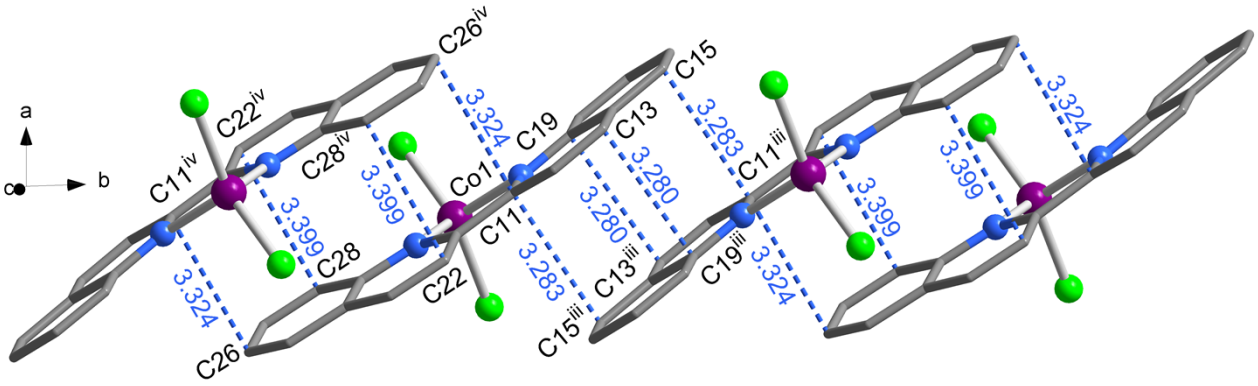

Fig. S7 The shortest C···C contacts [Å] between carbon atoms of 2,2'-biquinoline present in the crystal structure of **1**. Hydrogen atoms are omitted for clarity. Symmetry codes: (iii) 2 – x, 2 – y, – z; (iv) 2 – x, 1 – y, – z

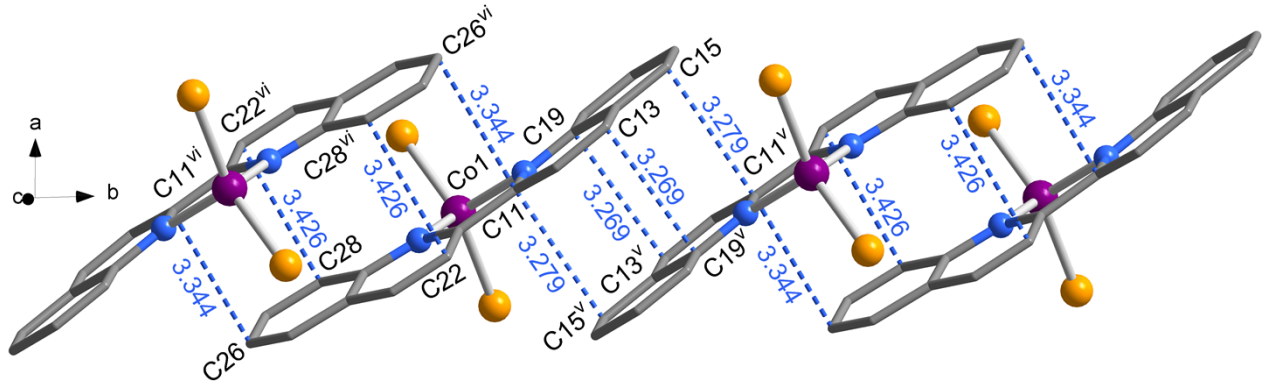

Fig. S8 The shortest C···C contacts [Å] between carbon atoms of 2,2'-biquinoline present in the crystal structure of **2**. Hydrogen atoms are omitted for clarity. Symmetry codes: (v) 1 – x, 1 – y, – z; (vi) 1 – x, – y, – z;

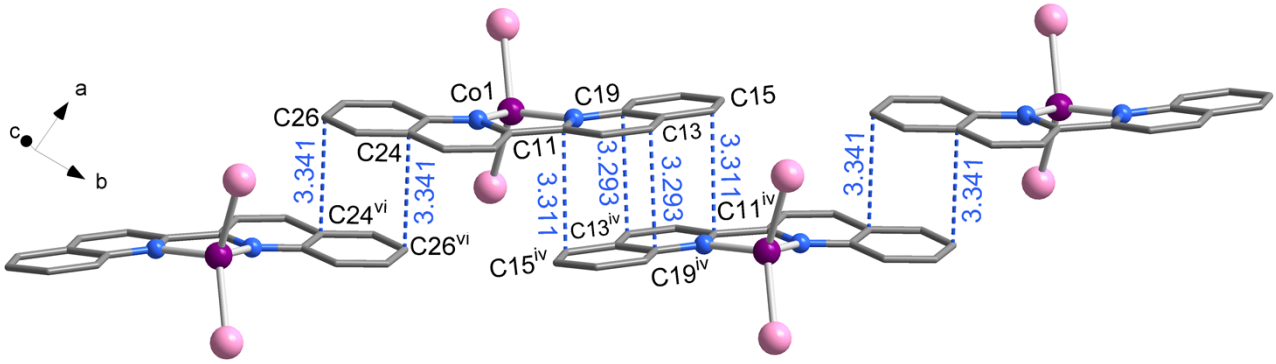

Fig. S9 The shortest C···C contacts [Å] between carbon atoms of 2,2'-biquinoline present in the crystal structure of **3**. Hydrogen atoms are omitted for clarity. Symmetry codes: (iv) 2 – x, 1 – y, – z; (vi) 1 – x, – y, – z;

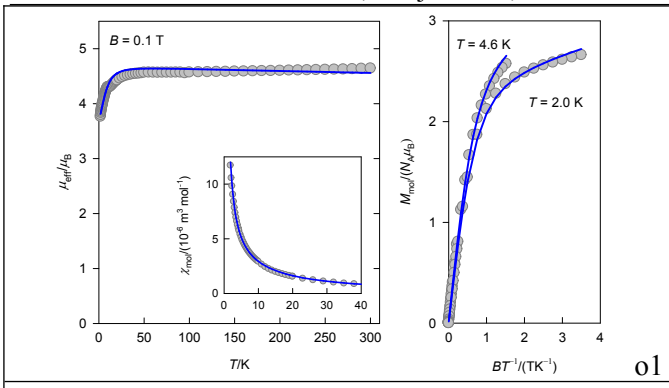

o1

DC susceptibiliy converted to the effective magnetic moment, and DC magnetization per formula unit

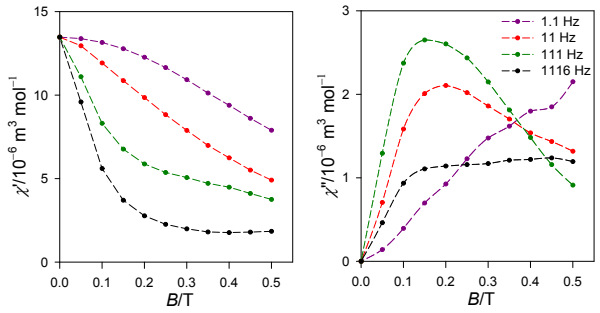

Field dependence of the AC susceptibility at T = 2.0 K for a set of frequencies of the AC field

B_{DC} = 0.2 T

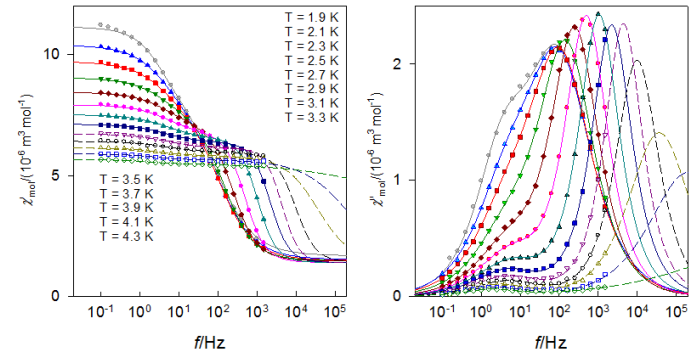

B_{DC} = 0.3 T

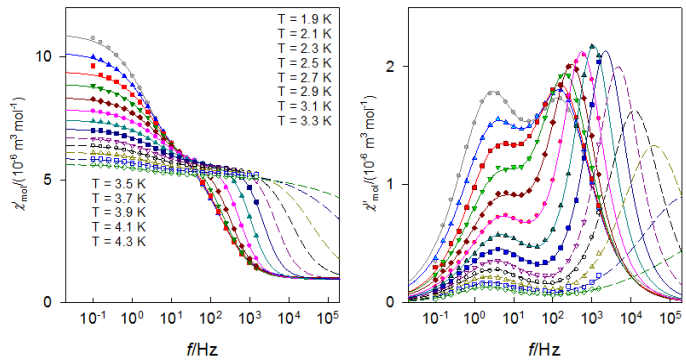

Left – in-phase AC susceptibility component; right – out-of phase AC susceptibility component

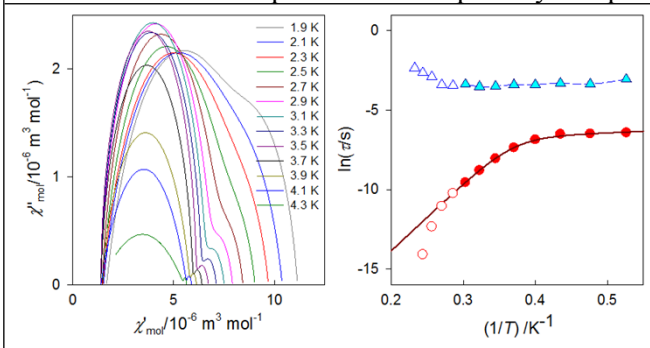

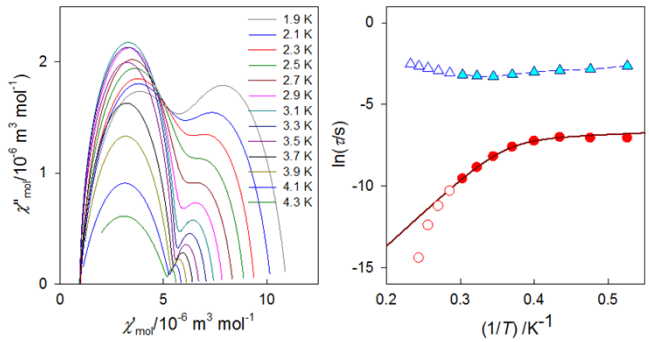

Left – Argand diagram, right – Arrhenius-like plot

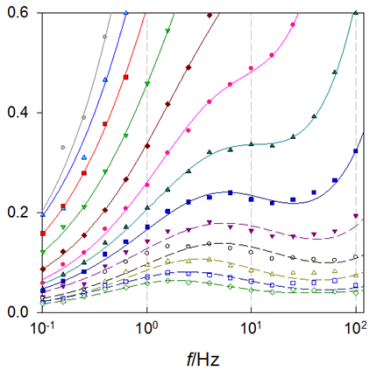

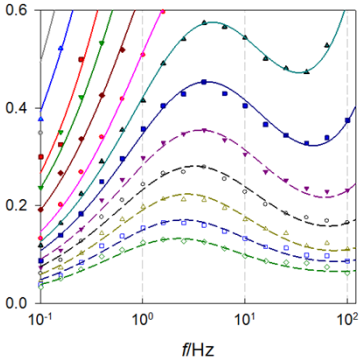

Zoomed out-of phase component

Fig. S10 Magnetic data for **1** = [Co(*biq*)Cl_2].

Two-component Debye model for AC susceptibility:
a) in phase susceptibility

$$\chi'(\omega) = \chi_S + (\chi_{T1} - \chi_S)\frac{1 + (\omega\tau_1)^{1-\alpha_1}\sin(\pi\alpha_1/2)}{1 + 2(\omega\tau_1)^{1-\alpha_1}\sin(\pi\alpha_1/2) + (\omega\tau_1)^{2-2\alpha_1}} + (\chi_{T2} - \chi_{T1})\frac{1 + (\omega\tau_2)^{1-\alpha_2}\sin(\pi\alpha_2/2)}{1 + 2(\omega\tau_2)^{1-\alpha_2}\sin(\pi\alpha_2/2) + (\omega\tau_2)^{2-2\alpha_2}}$$

b) out of phase susceptibility

$$\chi''(\omega) = (\chi_{T1} - \chi_S)\frac{(\omega\tau_1)^{1-\alpha_1}\cos(\pi\alpha_1/2)}{1 + 2(\omega\tau_1)^{1-\alpha_1}\sin(\pi\alpha_1/2) + (\omega\tau_1)^{2-2\alpha_1}} + (\chi_{T2} - \chi_{T1})\frac{(\omega\tau_2)^{1-\alpha_2}\cos(\pi\alpha_2/2)}{1 + 2(\omega\tau_2)^{1-\alpha_2}\sin(\pi\alpha_2/2) + (\omega\tau_2)^{2-2\alpha_2}}$$

for $\omega = 2\pi f$.

Table S11 Parameters of the extended Debye model for **1** (two relaxation processes) at B_{DC} = 0.2 T. [a]

T/K	χ_S	χ_{T1}	α_1	τ_1 /10^{-3} s	χ_{T2}	α_2	τ_2 /10^{-6} s	$R(\chi')$/%	$R(\chi'')$/%
1.9	1.67(6)	4.44(35)	0.20(3)	46.7(46)	11.14(3)	0.32(2)	1644(119)	0.64	1.8
2.1	1.52(3)	4.03(24)	0.30(2)	34.8(36)	10.39(2)	0.31(1)	1530(66)	0.23	1.2
2.3	1.48(2)	3.40(22)	0.32(2)	36.5(51)	9.70(2)	0.29(1)	1470(53)	0.32	0.72
2.5	1.47(3)	3.15(22)	0.33(4)	33.6(65)	9.03(3)	0.22(1)	1040(30)	0.44	1.8
2.7	1.46(3)	2.85(11)	0.31(3)	33.5(37)	8.44(2)	0.14(1)	630(10)	0.37	1.7
2.9	1.40(2)	2.60(5)	0.30(2)	20.6(17)	7.92(1)	0.07(1)	320(1)	0.29	0.87
3.1	1.40	2.41(2)	0.33(2)	29.5(13)	7.51(1)	0.04(1)	151(1)	0.26	0.71
3.3	1.40	2.17(3)	0.32(3)	34.4(29)	7.12(2)	0.04(1)	72(1)	0.45	1.2
3.5*	1.40	2.03(3)	0.36(3)	32.0(30)	6.73(1)	0.00(1)	36(1)	0.34	3.2
3.7*	1.40	1.86(3)	0.33(5)	33.6(43)	6.41(2)	0.07(2)	16(1)	0.42	4.8
3.9*	1.40	1.71(3)	0.26(7)	54.5(85)	6.13(1)	0.28(4)	4.37(74)	0.45	6.2
4.1*	1.40	1.64(3)	0.28(7)	70.4(121)	5.89(1)	0.41(6)	0.76(36)	0.35	8.9
4.3**	1.40	1.53(4)	0.17(16)	95(23)	5.65(1)	0.71(9)	0.0026(74)	0.39	6.5

[a] SI unit for the molar magnetic susceptibility [10^{-6} m^3 mol^{-1}]. Standard deviations in parentheses (last digit).
R – discrepancy factor of the fit for dispersion χ' and absorption χ'', respectively.
Notes to the fitting procedure
The fitting is considered as reliable when experimental data of χ'' pass through both maxima.
* If not, the points in the Arrhenius-like graph are marked by empty symbols and they do not enter the equation for the relaxation time. In such a case the adiabatic susceptibility χ_S becomes unstable during the fitting procedure and correlated with the isothermal susceptibility χ_{T1} for the first (faster) process; this needs be fixed either to the best estimate or to the zero.
** The fitting was finished for those temperatures when the standard deviations of parameters are higher than the absolute values of them.
Notice: 2.03(3) means 2.03 □ 0.03; 32.0(29) means 32.0 □ 2.9; 70.4(121) means 70.4 □ 12.1.

Table S12 Parameters of the extended Debye model for **1** (two relaxation processes) at B_{DC} = 0.3 T.

T/K	χ_S	χ_{T1}	α_1	τ_1 /10^{-3} s	χ_{T2}	α_2	τ_2 /10^{-6} s	$R(\chi')$/%	$R(\chi'')$/%
1.9	0.92(6)	6.14(21)	0.30(1)	70.9(31)	10.94(4)	0.29(2)	859(37)	0.53	2.4
2.1	0.97(2)	5.53(9)	0.32(1)	57.3(15)	10.19(2)	0.25(1)	862(15)	0.30	0.64
2.3	0.92(9)	4.37(33)	0.27(3)	53.8(59)	9.39(6)	0.25(3)	893(57)	1.3	1.2
2.5	0.93(3)	4.06(10)	0.31(1)	47.8(21)	8.90(2)	0.19(1)	715(12)	0.41	1.3
2.7	0.99(2)	3.73(7)	0.33(1)	41.4(16)	8.35(2)	0.12(1)	495(5)	0.33	1.5
2.9	0.95(2)	3.24(5)	0.32(1)	37.6(9)	7.86(1)	0.07(1)	276(2)	0.28	0.95
3.1	0.95(5)	2.86(6)	0.33(1)	38.3(11)	7.44(1)	0.04(1)	143(2)	0.33	0.81
3.3	0.95	2.49(3)	0.34(2)	41.2(16)	7.07(1)	0.05(1)	71.1(6)	0.40	1.9
3.5*	0.95	2.16(3)	0.34(2)	45.7(21)	6.72(2)	0.08(1)	33.4(6)	0.38	2.7
3.7*	0.95	1.89(4)	0.33(3)	52.8(44)	6.41(2)	0.21(3)	13.2(10)	0.57	5.2
3.9*	0.95	1.66(3)	0.30(3)	61.3(49)	6.11(2)	0.31(4)	4.11(71)	0.46	6.0
4.1*	0.95	1.48(4)	0.30(5)	69.4(82)	5.85(2)	0.50(7)	0.55(33)	0.46	8.7
4.3**	0.95	1.32(4)	0.27(5)	79.6(88)	5.61(1)	0.64(7)	0.032(42)	0.35	5.7

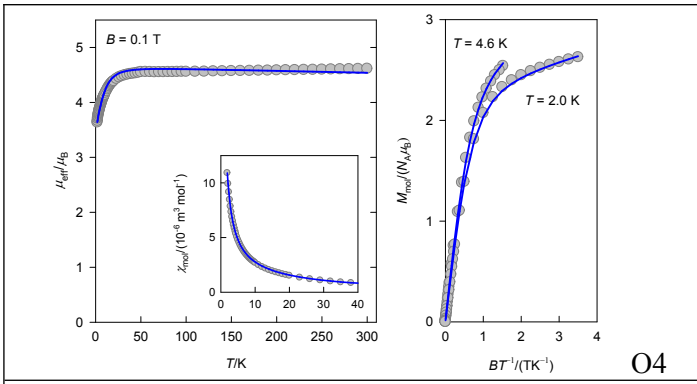

O4

DC susceptibiliy converted to the effective magnetic moment, and DC magnetization per formula unit

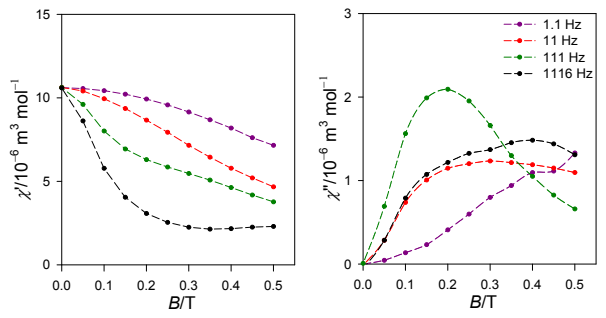

Field dependence of the AC susceptibility at T = 2.0 K for a set of frequencies of the AC field

B_{DC} = 0.2 T

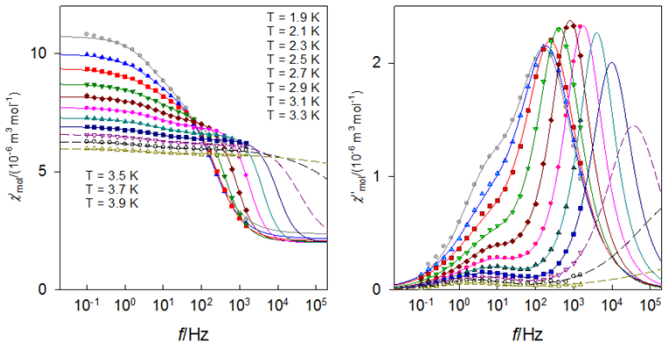

B_{DC} = 0.3 T

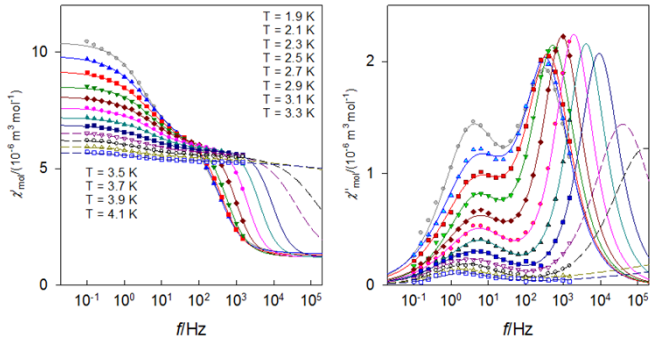

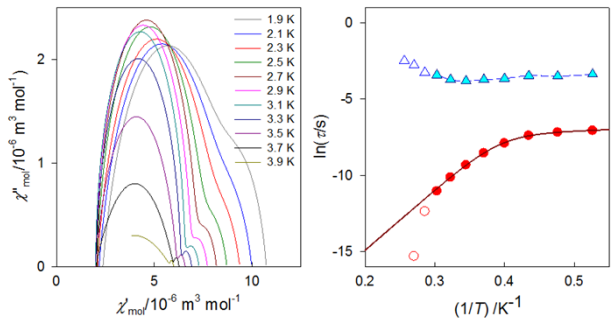

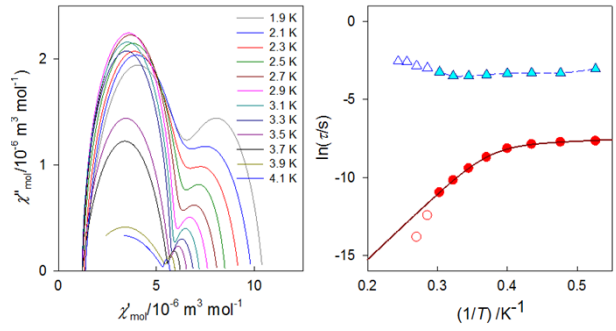

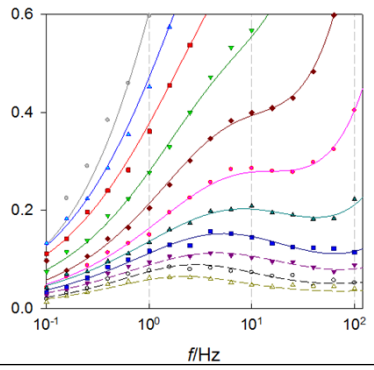

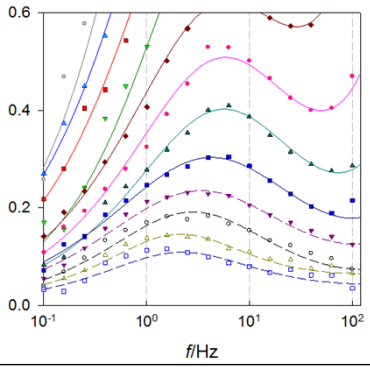

Zoomed out-of phase component

Fig. S11 Magnetic data for **2** = [Co(*biq*)Br_2].

Table S13 Parameters of the extended Debye model for **2** (two relaxation processes) at B_{DC} = 0.2 T.

T/K	χ_S	χ_{T1}	α_1	τ_1 /10^{-3} s	χ_{T2}	α_2	τ_2 /10^{-6} s	$R(\chi')$/%	$R(\chi'')$/%
1.9	2.40(5)	4.77(21)	0.25(3)	32.1(31)	10.74(2)	0.25(1)	830(30)	0.49	1.7
2.1	2.17(4)	4.06(20)	0.34(3)	30.5(45)	9.99(2)	0.24(1)	768(22)	0.37	1.4
2.3	2.08(3)	3.68(15)	0.36(3)	30.9(45)	9.37(2)	0.19(1)	622(11)	0.32	1.6
2.5	2.05(4)	3.44(11)	0.35(3)	25.7(31)	8.71(2)	0.10(1)	377(5)	0.37	1.8
2.7	2.05(4)	3.19(8)	0.34(3)	24.0(19)	8.18(1)	0.04(1)	197(2)	0.33	1.4
2.9	2.00	2.93(4)	0.37(3)	22.0(20)	7.72(2)	0.02(1)	89.1(7)	0.42	0.98
3.1	2.00	2.77(2)	0.40(2)	24.5(15)	7.29(1)	0.02(1)	39.4(4)	0.23	1.3
3.3	2.00	2.57(2)	0.38(3)	32.4(26)	6.91(1)	0.05(2)	16.4(6)	0.26	2.9
3.5*	2.00	2.42(3)	0.38(5)	41.6(60)	6.56(2)	0.20(5)	4.96(82)	0.35	4.8
3.7*	2.00	2.27(3)	0.29(7)	62(10)	6.26(1)	0.51(8)	0.22(19)	0.31	10
3.9**	2.00	2.14(6)	0.23(15)	82(14)	5.99(3)	0.80(11)	0.00002(16)	0.23	14

Table S14 Parameters of the extended Debye model for **2** (two relaxation processes) at B_{DC} = 0.3 T.

T/K	χ_S	χ_{T1}	α_1	τ_1 /10^{-3} s	χ_{T2}	α_2	τ_2 /10^{-6} s	$R(\chi')$/%	$R(\chi'')$/%
1.9	1.36(7)	5.53(16)	0.28(1)	46.5(21)	10.42(3)	0.19(2)	467(13)	0.67	2.2
2.1	1.36(5)	5.24(17)	0.36(2)	36.3(23)	9.85(4)	0.14(2)	437(10)	0.58	2.1
2.3	1.30(5)	4.47(13)	0.35(2)	36.5(22)	9.19(3)	0.13(1)	384(7)	0.55	1.9
2.5	1.22(5)	3.56(9)	0.28(1)	35.3(15)	8.51(2)	0.11(1)	291(4)	0.43	1.9
2.7	1.22(6)	3.35(9)	0.36(1)	32.6(14)	8.10(2)	0.06(1)	165(2)	0.36	1.9
2.9	1.22(13)	2.99(15)	0.35(1)	30.6(13)	7.62(2)	0.03(1)	81.5(29)	0.35	2.0
3.1	1.20	2.60(3)	0.35(1)	30.2(11)	7.20(1)	0.05(1)	38.4(5)	0.34	1.9
3.3	1.20	2.37(4)	0.40(2)	38.9(25)	6.89(2)	0.06(2)	17.3(8)	0.40	4.8
3.5*	1.20	2.07(4)	0.38(3)	49.9(42)	6.55(2)	0.27(5)	4.00(80)	0.43	4.7
3.7*	1.20	1.84(3)	0.32(3)	58.3(46)	6.22(1)	0.35(7)	1.00(49)	0.36	7.2
3.9**	1.20	1.58(7)	0.25(7)	75.2(74)	5.96(3)	0.76(10)	0.00078(288)	0.33	8.5
4.1**	1.20	1.48(10)	0.25(12)	77.5(117)	5.71(6)	0.80(21)	0.00001(17)	0.40	14

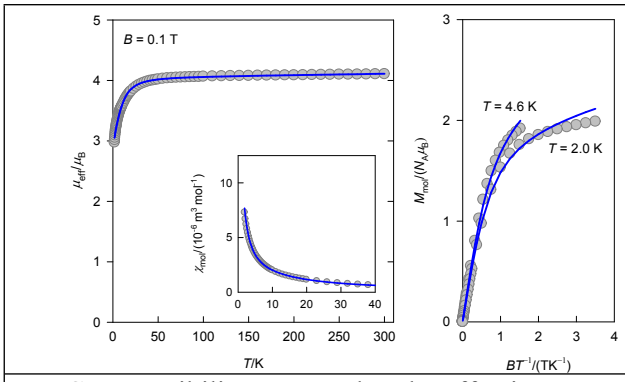

DC susceptibiliy converted to the effective magnetic moment, and DC magnetization per formula unit

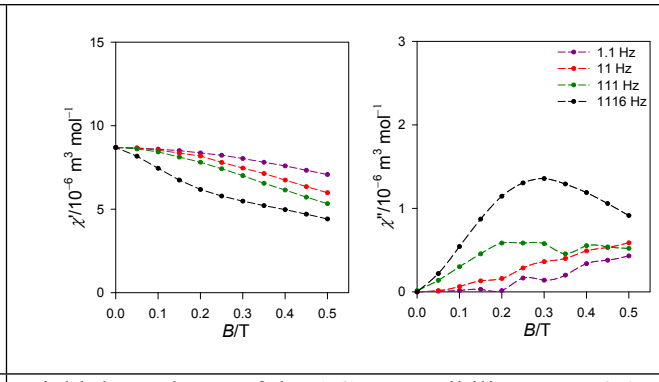

Field dependence of the AC susceptibility at $T = 2.0$ K for a set of frequencies of the AC field

$B_{DC} = 0.2$ T

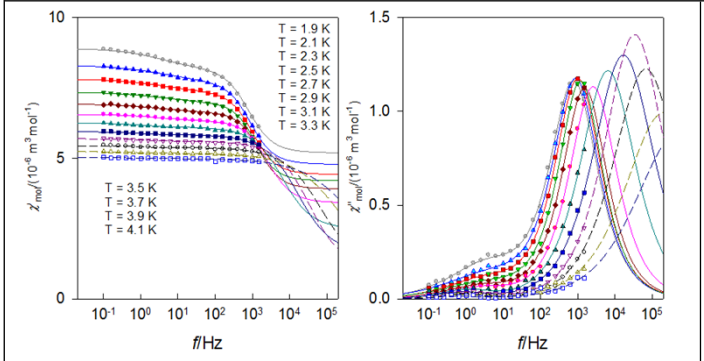

$B_{DC} = 0.3$ T

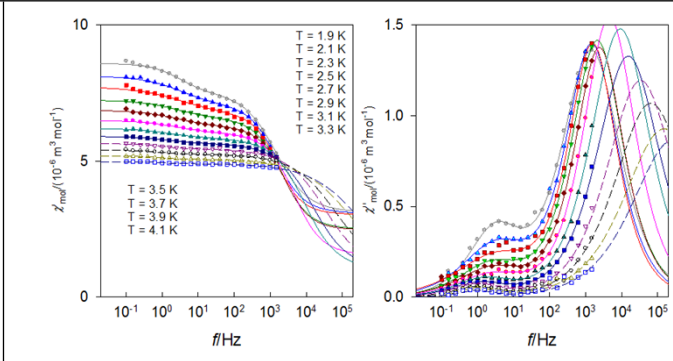

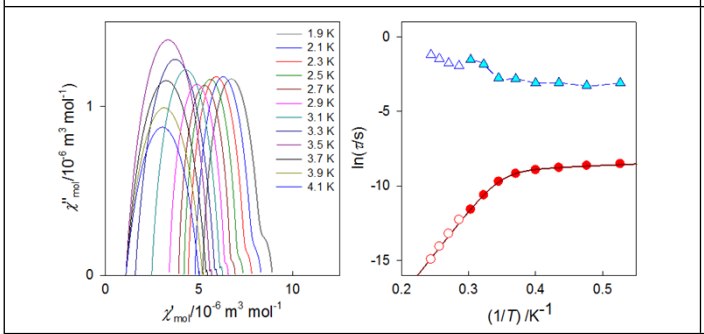

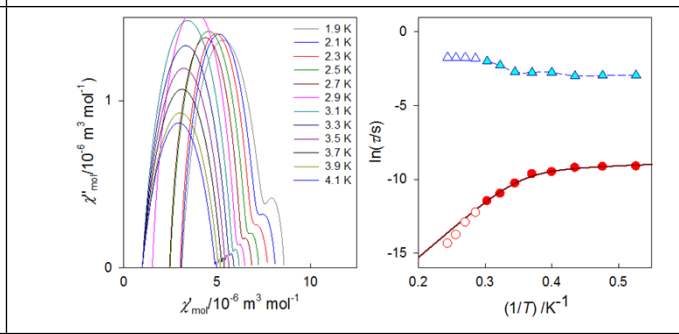

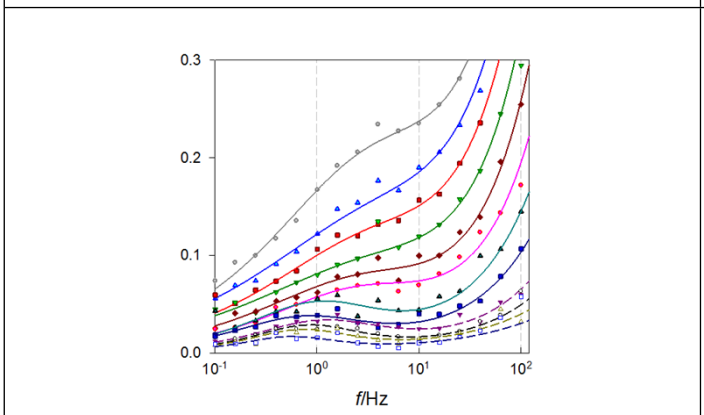

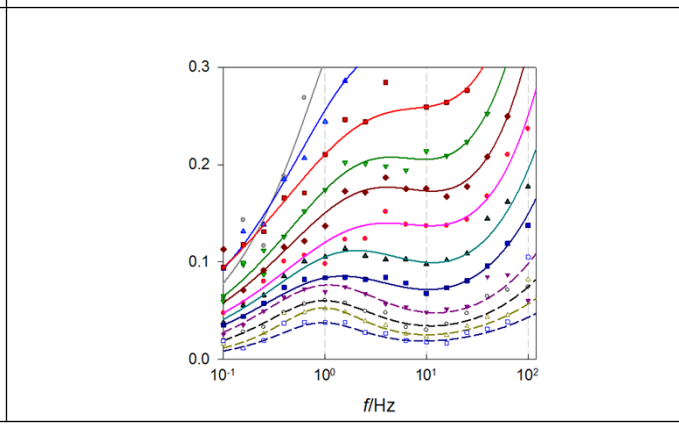

Zoomed out-of phase component

Fig. S12 Magnetic data for **3** = [Co(*biq*)I_2].

Table S15 Parameters of the extended Debye model for **3** (two relaxation processes) at B_{DC} = 0.2 T.

T/K	χ_S	χ_{T1}	α_1	τ_1 /10^{-3} s	χ_{T2}	α_2	τ_2 /10^{-6} s	$R(\chi')$/%	$R(\chi'')$/%
1.9	5.19(5)	5.93(10)	0.42(5)	45.4(75)	8.91(2)	0.17(2)	201(5)	0.26	2.2
2.1	4.78(5)	5.40(12)	0.49(6)	37.9(11)	8.31(3)	0.15(2)	178(4)	0.28	1.9
2.3	4.42(5)	4.87(9)	0.44(6)	46.0(98)	7.81(2)	0.15(1)	155(4)	0.25	1.4
2.5	4.19(6)	4.60(10)	0.49(8)	45.4(135)	7.36(2)	0.12(2)	133(4)	0.25	2.4
2.7	3.91(7)	4.19(9)	0.41(7)	59.7(130)	6.93(1)	0.13(1)	103(4)	0.26	1.3
2.9	3.42(10)	3.63(11)	0.35(6)	64.2(105)	6.56(1)	0.17(1)	61.2(36)	0.17	2.1
3.1*	2.47(46)	2.61(47)	0.22(12)	160(38)	6.25(1)	0.25(2)	24.6(58)	0.26	3.7
3.3*	1.60	1.70(2)	0.23(14)	215(63)	5.94(1)	0.30(1)	9.38(43)	0.28	3.5
3.5*	1.10	1.18(1)	0.16(15)	141(41)	5.67(1)	0.29(2)	4.69(41)	0.32	3.8
3.7*	1.10	1.16(1)	0.09(17)	170(49)	5.44(1)	0.37(2)	1.85(28)	0.26	7.7
3.9*	1.10	1.15(1)	0.04(20)	230(73)	5.23(1)	0.42(2)	0.784(179)	0.23	12
4.1*	1.10	1.13(1)	0	300(226)	5.02(1)	0.56(5)	0.334(201)	0.45	18

Table S16 Parameters of the extended Debye model for **3** (two relaxation processes) at B_{DC} = 0.3 T.

T/K	χ_S	χ_{T1}	α_1	τ_1 /10^{-3} s	χ_{T2}	α_2	τ_2 /10^{-6} s	$R(\chi')$/%	$R(\chi'')$/%
1.9	3.11(19)	4.20(24)	0.26(4)	51.8(43)	8.59(2)	0.30(2)	110(9)	0.45	2.5
2.1	3.08(15)	4.14(20)	0.38(4)	51.2(61)	8.13(3)	0.30(2)	107(7)	0.38	3.1
2.3	3.03(22)	4.02(31)	0.45(6)	49.8(121)	7.73(5)	0.19(4)	100(9)	0.64	2.7
2.5	2.49(14)	3.16(17)	0.37(3)	63.1(62)	7.24(1)	0.23(2)	75.2(48)	0.30	1.6
2.7	2.46(21)	3.06(24)	0.38(5)	62.7(92)	6.87(2)	0.21(2)	65.4(64)	0.38	2.7
2.9	1.53(37)	2.01(39)	0.38(5)	65.1(89)	6.50(2)	0.23(2)	34.5(52)	0.29	2.2
3.1*	1.0	1.34(3)	0.32(7)	101(17)	6.19(2)	0.30(1)	17.4(6)	0.36	4.2
3.3*	1.0	1.25(3)	0.30(9)	134(29)	5.91(2)	0.24(2)	10.4(6)	0.41	4.1
3.5*	1.0	1.19(3)	0.20(13)	162(42)	5.64(2)	0.37(3)	4.74(67)	0.49	10.9
3.7*	1.0	1.14(2)	0.13(9)	175(29)	5.40(1)	0.41(2)	2.45(31)	0.28	8.3
3.9*	1.0	1.10(1)	0.00(13)	172(33)	5.18(1)	0.46(3)	1.05(25)	0.34	11.7
4.1*	1.0	1.07(1)	0.00(20)	176(50)	4.98(1)	0.47(4)	0.583(228)	0.25	25.5

DC magnetic data fitting procedure

Spin Hamiltonian of the form

$$\hat{H}_{k,l} = D(\hat{S}_z^2 - \hat{S}^2/3)\mathsf{h}^{-2} + E(\hat{S}_x^2 - \hat{S}_y^2)\mathsf{h}^{-2}$$
$$+\mu_\mathrm{B} B_m (g_x \sin\vartheta_k \cos\varphi_l \hat{S}_x + g_y \sin\vartheta_k \sin\varphi_l \hat{S}_y + g_z \cos\vartheta_k \hat{S}_z)\mathsf{h}^{-1}$$

has been applied in interpreting the magnetic data. The zero-field splitting (ZFS) is described by two parameters: D – the axial ZFS parameter, and E – the rhombic ZFS one, respectively. The Zeeman term needs averaging over a number of grid points (k, l) distributed uniformly over a sphere (210 points at the top hemisphere). The generated energy levels for three magnetic fields B_m enter the partition function from which the magnetization and magnetic susceptibility are obtained through the formulae of the statistical thermodynamics. The susceptibility data were corrected for the molecular-field correction (zj) and the temperature-independent magnetism χ_TIM

$$\chi_\mathrm{corr} = \chi_\mathrm{mol}/[1-(zj)\chi_\mathrm{mol}] + \chi_\mathrm{TIM}$$

The latter term accounts for the uncompensated underlying diamagnetism and the temperature-independent paramagnetism, along with the signal of the sample holder. The susceptibility and magnetization data sets have been fitted simultaneously by applying a joint error functional

$$F_2 = w_1\left[(1/N)\sum_i^N \left|\frac{\chi_i^\mathrm{c} - \chi_i^\mathrm{o}}{\chi_i^\mathrm{o}}\right|\right] + w_2\left[(1/K)\sum_j^K \left|\frac{M_j^\mathrm{c} - M_j^\mathrm{o}}{M_j^\mathrm{o}}\right|\right]$$

where w_1 and w_2 are postulated weights of the two data-sets. An advanced fitting procedure using a genetic algorithm has been applied.

DC magnetic data fitting with final negative *D* values

Table S17 Spin Hamiltonian parameters

Complex	g_{iso}	D/hc /cm^{-1}	E/hc /cm^{-1}	χ_{TIM} /10^{-9} m^3 mol^{-1}	zj/hc /cm^{-1}	$R(\chi)$	$R(M)$
1	2.444	–9.00	-	–10.99	–0.02	0.046	0.025
2	2.363	–11.52	-	–4.12	–0.01	0.015	0.056
3	2.112	–9.25	-	–0.69	–0.04	0.011	0.042

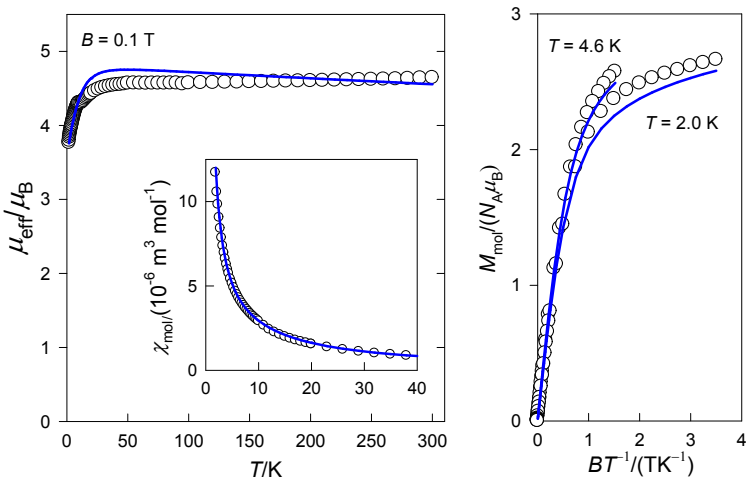

Fig. S13 Best negative *D*-value fit of the DC magnetic data for **1**.

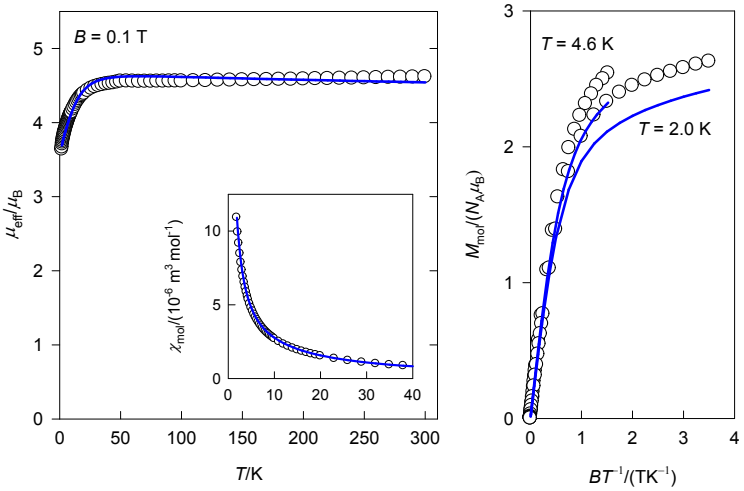

Fig. S14 Best negative *D*-value fit of the DC magnetic data for **2**.

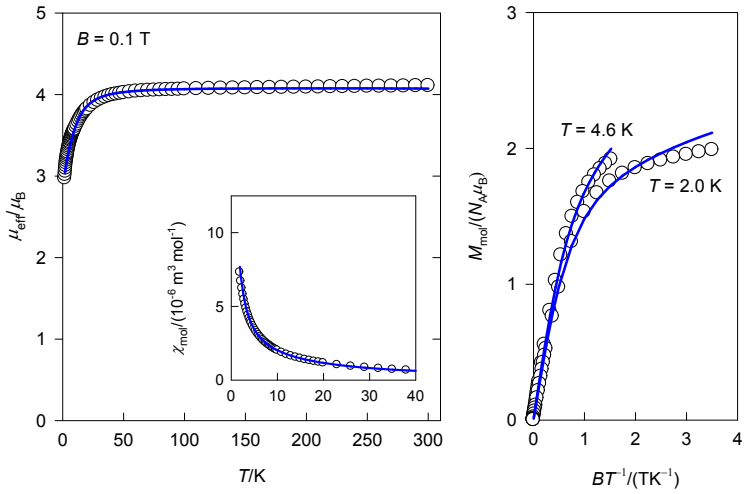

Fig. S15 Best negative *D*-value fit of the DC magnetic data for **3**.

Magnetic hyperfine structure for complex 1

```
 ------------------------------------------------------------
 Nucleus   0Co: A:ISTP=   59 I=  3.5 P=125.8968 MHz/au**3
           Q:ISTP=   59 I=  3.5 Q=  0.3800 barn
 ------------------------------------------------------------
 ZORA HFC tensor (only A(iso) and A(dip) are corrected)
 Raw HFC matrix (all values in MHz):
        -36.7006     51.9452     -3.8193
         52.0685   -116.3598    -19.2705
         -3.8466    -19.2553    -40.5104

 A(FC)   -132.4420   -132.4420   -132.4420
 A(SD)     45.2099     16.9425    -62.1524
 A(SO)     80.6611     72.8958     50.1981  A(PC) =    67.9183
 ____________________________________________
 A(Tot)    -6.5709    -42.6036   -144.3963  A(iso)=   -64.5236

 Orientation:
  X      0.8215471  -0.3796460  -0.4253579
  Y      0.4502755  -0.0256002   0.8925226
  Z     -0.3497319  -0.9247776   0.1499135
```

Magnetic hyperfine structure for complex 2

```
 ------------------------------------------------------------
 Nucleus   2Co: A:ISTP=   59 I=  3.5 P=125.8968 MHz/au**3
           Q:ISTP=   59 I=  3.5 Q=  0.3800 barn
 ------------------------------------------------------------
ZORA HFC tensor (only A(iso) and A(dip) are corrected)
 Raw HFC matrix (all values in MHz):
        -28.6726    -50.9393      3.8706
        -51.5344   -104.4478    -19.9140
          4.2836    -20.0672    -35.8193

 A(FC)   -128.5796   -128.5796   -128.5796
 A(SD)     40.8689     14.8904    -55.7592
 A(SO)     89.3705     76.0472     51.3815  A(PC) =    72.2664
 ____________________________________________
 A(Tot)     1.6597    -37.6421   -132.9573  A(iso)=   -56.3132

 Orientation:
  X      0.8217454   0.3755206   0.4286243
  Y     -0.4591949  -0.0090572   0.8882894
  Z      0.3374531  -0.9267698   0.1649945
```

Magnetic hyperfine structure for complex 3

Nucleus 2Co: A:ISTP= 59 I= 3.5 P=125.8968 MHz/au**3
Q:ISTP= 59 I= 3.5 Q= 0.3800 barn

ZORA HFC tensor (only A(iso) and A(dip) are corrected)
Raw HFC matrix (all values in MHz):

-10.3378	-51.5964	5.3985
-53.5521	-88.6422	-20.9859
6.8063	-22.2006	-25.2497

A(FC)	-122.1247	-122.1247	-122.1247		
A(SD)	36.0416	12.7297	-48.7713		
A(SO)	107.1352	82.1614	52.8478	A(PC) =	80.7148
A(Tot)	21.0521	-27.2336	-118.0482	A(iso)=	-41.4099

Orientation:

X	0.8068735	0.4155197	0.4198792
Y	-0.4552053	-0.0156526	0.8902489
Z	0.3764882	-0.9094495	0.1765171

Table S18 Mononuclear Co(II) SMMs with positive *D* values

Compound	Chromophore	D /cm^{-1}	U /cm^{-1} (B_{DC} /T)	Ref.
[CoL1Cl_2]	{CoN_3Cl_2}	151	9.4 (0.1)	[1]
[Co(*terpy*)Cl_2]	{CoN_3Cl_2}	100	19.4 (0.06)	[2]
cis-[Co(*dmphen*)$_2$(NCS)$_2$]	{CoN_6}	98	18.1 (0.25)	[3]
[Co(*acac*)$_2$(H_2O)$_2$]	{CoO_6}	57	~14 - 17	[4]
[Co(*abpt*)$_2$(*tcm*)$_2$]	{CoN_6}	48	59.9 (0.3)	[5]
[Co(μ-L2)(μ-OAc) Y(NO_3)$_2$]	{CoO_3N_3}	41.7	15.7 (0.1)	[6]
[Co(H_2*dapb*)(H_2O)(NO_3)](NO_3)	{CoO_4N_3}	32.4	56.3 (0.1)	[7]
[(L3)$_4$$Co^{II}Co^{III}_2$($H_2O$)$_2$]($NO_3$)	{CoO_4N_2}	31.9	5.6 (0.1)	[8]
[Co(*dapb*)(*im*)$_2$]·H_2O	{CoO_2N_5}	24.8	62.3 (0.1)	[7]
[CoL4(H_2O)$_2$]Cl_2·4H_2O	{CoO_2N_5}	24.6	20.7 (0.1)	[7]
K[Co(N[$CH_2C(O)NC(CH_3)_3$]$_3$)]	{CoN_4}	16	8.7 (0.15)	[9]
[CoL5Cl_2(MeCN)]	{$CoONCl_2$}	15.6	10.3 (0.25)	[10]
[CoCl(3G)](CF_3SO_3)	{CoN_3Cl}	12.7	24 (0.15)	[11]
[CoL5Br_2(MeCN)]	{$CoONBr_2$}	11.2	8.2 (0.25)	[10]
[Co(*dmphen*)Br_2]	{CoN_2Br_2}	10.6	22.9 (0.1)	[12]

L1 = 4‘-1-heptynyl-2‘,6‘-dipyrazolyl-pyridine; *terpy* = terpyridine; *dmphen* = 2,9-dimethyl-1,10-phenanthroline; *abpt* = 4-amino-3,5-bis(2-pyridyl)-1,2,4-triazole; tcm = tricyanomethanide anion; H2L2 = N,N’,N’’-trimethyl-N,N’’-bis(2-hydroxy-3-methoxy-5-methylbenzyl)-diethylenetriamine; H2dapb = 2,6-diacetylpyridine bis(benzoyl hydrazine; HL3 = (E)-N'-(pyridin-2-ylmethylene)pyrazine-2-carbohydrazide; L4 = 2,13-dimethyl-3,6,9,12-tetraaza-1(2,6)-pyridinacyclotridecaphane-2,12-diene, im = imidazole; L5 = 2,3-diphenyl-1,2,3,4-tetrazolium-5-olate; 3G = 1,1,1-tris-[2N-(1,1,3,3-tetramethylguanidino)methyl]ethane.

References:

[1] C. Rajnak, J. Titis, O. Fuhr, M. Ruben, R. Boca, Inorg. Chem. 53 (2014)8200–8202.

[2] F. Habib, O.R. Luca, V. Vieru, M. Shiddiq, I. Korobkov, S.I. Gorelsky, M.K. Takase,L.F. Chibotaru, S. Hill, R.H. Crabtree, M. Murugesu, Angew. Chem. Int. Ed. Engl.52 (2013) 11290–11293.

[3] J. Vallejo, I. Castro, R. Ruiz-Garcia, J. Cano, M. Julve, F. Lloret, G. De Munno, W. Wernsdorfer, E. Pardo, J. Am. Chem. Soc., 134 (2012) 15704-15707.

[4] S. Gomez-Coca, A. Urtizbarea, E. Cremades, P.J. Alonso, A. Camón, E. Ruiz, F. Luis, Nat. Commun., 5 (2014) 4300.

[5] R. Herchel, L. Váhovská, I. Potocnák, Z. Trávnícek, Inorg. Chem., 53 (2014) 5896-5898.

[6] E. Colacio, J. Ruiz, E. Ruiz, E. Cremades, J. Krzystek, S. Carretta, J. Cano, T. Guidi, W. Wernsdorfer, E.K. Brechin, Angew. Chem. Int. Ed., 52 (2013) 9130-9134.

[7] X.-C. Huang, C. Zhou, D. Shao, X.-Y. Wang, Inorg. Chem., 53 (2014) 12671-12673.

[8] D. Wu, X. Zhang, P. Huang, W. Huang, M. Ruan, Z.W. Ouyang, Inorg. Chem., 52 (2013) 10976-10982.

[9] S. Gómez-Coca, E. Cremades, N. Aliaga-Alcalde, E. Ruiz, J. Am. Chem. Soc., 135 (2013) 7010-7018.

[10] S. Vaidya, A. Upadhyay, S.K. Singh, T. Gupta, S. Tewary, S.K. Langley, J.P.S. Walsh, K.S. Murray, G. Rajaraman, M. Shanmugam, Chem. Commun., Chem. Commun., 2015, 51, 3739 - 3742.

[11] J.M. Zadrozny, J. Liu, N.A. Piro, C.J. Chang, S. Hill, J.R. Long, Chem. Commun., 48 (2012) 3927-3929.

[12] W. Huang, T. Liu, D. Wu, J. Cheng, Z.W. Ouyang, C. Duan, Dalton Trans., 42 (2013) 15326-15331.